Regulation of the long noncoding RNA XIST on the inflammatory polarization of microglia in cerebral infarction

MIN ZHANG[1], JIAN-KAI YANG[2] and JING MA[3]

[1]Department of Neurosurgery, The Second Affiliated Hospital of Xingtai Medical College, Xingtai, Hebei 054000; [2]Department of Neurosurgery, The Second Hospital of Hebei Medical University, Shijiazhuang, Hebei 050000; [3]Meteorological Service and Applied Meteorology, Ren County Meteorological Bureau of Hebei Province, Xingtai, Hebei 055150, P.R. China

Received June 14, 2020; Accepted March 22, 2021

DOI: 10.3892/etm.2021.10356

Abstract. Proinflammatory polarization of microglia aggravates brain injury in cerebral infarction. The present study focused on the role of long non-coding (lnc)RNA X-inactive specific transcript (XIST) in the phenotype modulation of microglia. It was revealed that lncRNA XIST was significantly upregulated in both a mouse cerebral infarction model induced by middle cerebral artery occlusion (MCAO) and an activated microglial model induced by oxygen/glucose deprivation (OGD). The overexpression of XIST enhanced the expression and release of pro-inflammatory mediators [such as tumor necrosis factor (TNF)-α, IL-6, and iNOS] in microglia. Culture supernatant from lncRNA XIST-overexpressed microglial cells induced the apoptosis of primary neurons, while TNF-α antibody counteracted this neurotoxic effect. LncRNA XIST served as a sponge for miR-96-5p, counteracting its inhibitory effect on IKKβ/NF-κB signaling and TNF-α production. Notably, TNF-α was positively regulated by XIST and in turn enhanced XIST expression in microglia. The lncRNA XIST-TNF-α feedback promoted the proinflammatory polarization of microglia, thereby exacerbating cerebral neuron apoptosis.

Introduction

Cerebral infarction is one of the leading causes of long-term disability and death worldwide (1), accounting for more than 75% of all stroke cases (2). Cerebral infarction occurs when blood flow to the brain is blocked, resulting in hypoxia and the rapid death of cerebral tissues. The factors that induce cerebral infarction are complex, including genetic and environmental factors (3,4). Continuous efforts have been made to elucidate its mechanism and to find appropriate therapeutic targets. Recently, studies have revealed the crucial role of brain-resident immune cells in regulating the progression of cerebral infarction, indicating that targeting these immune cells may be an attractive therapeutic strategy (5,6).

Microglial cells are the first line of defense of the host against ischemic injury (5,7). After brain injury, microglia are rapidly activated. Activated microglia can secrete a variety of factors to regulate inflammation. Among them, microglia releasing pro-inflammatory mediators [such as tumor necrosis factor (TNF)-α, interleukin (IL)-1β and interferon (IFN)-γ] are defined as the M1-type, while those releasing neuroprotective factors (such as IL-4, IL-10 and TGF-β) are defined as the M2-type (8,9). The polarization of activated microglia into the M1 or M2 type depends on a variety of molecular signals in the microenvironment. For example, IFN-γ, TNF-α, IL-2, and lipopolysaccharide promote the polarization of microglia into the M1 type. However, chondroitin sulfate, proteoglycan and IL-4 promote the polarization of microglia into into the M2 type (9,10). Therefore, targeting microglial activation is considered as a promising therapeutic strategy in the treatment of cerebral infarction.

Long non-coding (lnc) RNAs, as noncoding transcripts longer than 200 bp, play pivotal roles in various biological and pathological processes, including cerebral infarction (11,12). Multiple lncRNAs have been revealed to regulate the progression of ischemic infarction (13). For instance, lncRNA MEG3 modulated neuronal death following cerebral infarction via miR21/PDCD4 signaling (14). LncRNA H19 contributed to microglial polarization to the M1 phenotype, giving rise to post-stroke neuroinflammation (15). However, research on the role of lncRNAs in cerebral infarction and their underlying mechanisms remain at an early stage (12). Recently, lncRNA X-inactive specific transcript (XIST) has been reported to be involved in several neurological diseases, such as spinal cord injury (16). However, the role of XIST in cerebral ischemia is unclear.

In the present study, it was hypothesized that XIST plays an important role in regulating the inflammatory polarization of microglial cells in cerebral infarction and the role of the lncRNA XIST in microglial phenotype modulation was explored using

Correspondence to: Dr Min Zhang, Department of Neurosurgery, The Second Affiliated Hospital of Xingtai Medical College, 618 Gangtie Bei Road, Xingtai, Hebei 054000, P.R. China
E-mail: zhangmin22000@163.com

Key words: long non-coding RNA X-inactive specific transcript, microglia, microRNA-96-5p, inhibitor of nuclear factor κB kinase subunit β, tumor necrosis factor-α

an *in vitro* oxygen-glucose deprivation (OGD) model and an *in vivo* middle cerebral artery occlusion (MCAO) model.

Materials and methods

Establishment of cerebral infarction animal model. A total of 24 male C57BL/6 mice (6-8 weeks old; weighing 20±0.3 g) were purchased from SLAC Laboratory Animal Co., Ltd. All experiments were carried out in accordance with the National Institutes of Health (NIH) guidelines for the care and use of laboratory animals and were approved by the Animal Ethics Committee of Xingtai Medical College Second Affiliated Hospital (Xingtai, China). Mice were fed with food and water *ad libitum* and were kept at 24±2˚C and 55±2% humidity, alternating between light and dark for 12 h. Mice were randomly divided into two groups: Sham group and the cerebral infarction group. A total of 12 mice were placed in each group. A cerebral infarction animal model was established using the MCAO method according to previously reported methods (17,18). Mice were anesthetized by intraperitoneal injection of 5% chloral hydrate (300 mg/kg). Briefly, common, internal and external carotid arteries were exposed after mice were anesthetized and a nylon suture was then inserted. Thereafter, the middle cerebral artery (MCA) was occluded using the nylon suture after moving it forward to the origin of the MCA. Mice in the sham operation group were only treated with neck incision and suture after separation, without vascular ligation. At the end of the experiment, mice were anesthetized with chloral hydrate and then euthanized by cervical dislocation. Three mice were randomly sacrificed in each group at 12, 36, 96 and 168 h after MCA or Sham surgery respectively before the cerebral tissues obtained for further investigation.

Cell culture and oxygen/glucose deprivation (OGD) treatment. The mouse microglial cell line, BV-2, was obtained from the Cell Bank of Chinese Academy of Sciences and cultured in DMEM (Gibco; Thermo Fisher Scientific, Inc.) containing 10% fetal bovine serum (FBS; Gibco; Thermo Fisher Scientific, Inc.) at 37˚C and 5% CO_2. A total of two pregnant female C57BL/6 mice (10-12 weeks old; weighing 20±0.3 g) were purchased from SLAC Laboratory Animal Co., Ltd.. Mice were fed with food and water *ad libitum*, and were kept at 24±2˚C and 55±2% humidity, in alternating between light and dark for 12 h, whilst waiting until the pregnant mice to give birth. Primary neurons were isolated from the cerebral cortices of C57BL/6 mice within 24 h of birth as previously described and cultured in neurobasal media (Gibco; Thermo Fisher Scientific, Inc.) supplemented with 2% B-27 (Gibco; Thermo Fisher Scientific, Inc.) at 37˚C and 5% CO_2 (19).

For OGD treatment, BV-2 cells were incubated in serum/glucose-free DMEM under the culture conditions of 94% N_2/5% CO_2/1% O_2 and 37˚C for 2 h and then returned to normal culture conditions. Subsequently, 24 h after BV-2 cells returned to normal culture conditions, the culture supernatants of BV-2 cells were collected and used as the conditioned media used to treat neurons for 12, 36 and 48 h at 37˚C.

Cell transfection. LncRNA XIST and inhibitor of nuclear factor κB kinase subunit β (IKKβ) cDNAs were cloned into the pXJ40-HA-Merlin I (Addgene plasmid no. 19699; http://n2t.net/addgene:19699; RRID:Addgene_19699) to construct over-expression vectors. Small interfering (si)RNA-XIST, short hairpin (sh)RNA-IKKβ, microRNA (miR)-96-5p mimics, and miR-96-5p inhibitor were purchased from Shanghai GenePharma Co., Ltd. All small RNA sequences are as follows: siRNA-XIST, 5'-AUAACAGUAAGUCUGAUAGAG GACA-3'; shRNA-IKKβ, 5'-CACCGTCTTGTCGCCTAG AGCTATTCAAGAGATAGCTCTAGGCGACAAGACTTT TTTG-3'; miR-96-5p mimics, 5'-UUUGGCACUAGCACA UUUUUGCU-3'; miR-96-5p inhibitor, 5'-AGCAAAAAU GUGCUAUGUGCCAAA-3'; siRNA negative control, 5'-UUA CUCAUGUGUCAUAACACAGGUG-3'; shRNA negative control, 5'-CCTAAGGTTAAGTCGCCCTCGCTCGAGCGA GGGCGACTTAACCTTAGG-3'; mimic negative control, 5'-UUCUCCGAACGUGUCACGUTT-3'; inhibitor negative control, 5'-UUGUACUACACAAAAGUACUG-3'.

BV-2 cells were seeded in 96-well plates at $5x10^4$ cells/well. LncRNA XIST overexpression vector/siRNA, miR-96-5p mimics/inhibitor, IKKβ overexpression vector/shRNA and corresponding controls were transfected into BV-2 cells using Lipofectamine® 2000 (Invitrogen; Thermo Fisher Scientific, Inc.) according to the manufacturer's instructions, respectively. Briefly, 5 μl transfection reagent and 0.5 μg plasmid or 5 pmol small RNA were mixed in 50 μl serum-free DMEM, left to stand for 5 min and then mixed. Following incubation at room temperature for 20 min, the mix was added to serum-starved cells and incubated at 37˚C for 4 h. Following this, 48 h later, cells and the culture supernatants were harvested for relative assays.

ELISA. After 24-h transfection, BV-2 cells (seeded in 96-well plates at $5x10^4$ cells/well) were exposed to the OGD treatment. Then TNF-α (cat. no. ab181421; Abcam) and IL-6 (cat. no. ab222503; Abcam) levels in cell culture supernatants were examined using ELISA kits. The absorbance was detected at 450 nm using a microplate reader (Tecan Group, Ltd.).

Flow cytometry. Cell expression levels of inducible nitric oxide synthase (iNOS) were detected by flow cytometry after BV-2 cells were subjected to transfection and OGD treatment. In brief, BV-2 cells were fully digested using 0.25% trypsin at 37˚C for 5 min. After cell counting, cells were resuspended at a density of 100 μl 4% formaldehyde per $1x10^6$ cells and fixed at room temperature for 15 min. Ice-cold 100% methanol was then slowly added to a final concentration of 90% methanol and permeabilized on ice for 10 min. The methanol was subsequently separated by centrifugation at 500 x g for 5 min at room temperature, and followed by incubation with 2 ng/ml PE-Cyanine7-labeled iNOS antibody (cat. no. 25-5920-80; eBioscience; Thermo Fisher Scientific, Inc.) in the dark at room temperature for 20 min. After rinsing three times with PBS, these cells were were detected by a flow cytometer (BD FACSCalibur™; BD Biosciences) and analyzed using FlowJo v10 software (FlowJo, LLC).

Lactate dehydrogenase (LDH) assay. The neurons were seeded into 96-well plates ($5x10^4$ cells/well) and stimulated with OGD-treated BV-2 cell conditioned media. In total, 5 ng/ml TNF-α neutralizing antibody (cat. no. 7321; Cell Signaling Technology, Inc.) or its IgG control (cat. no. 3900;

Cell Signaling Technology, Inc.) were added, before the cells were incubated at 37˚C and 5% CO_2 for 24 h. LDH released from apoptotic and necrotic neurons was examined by an LDH assay kit in accordance with the manufacturer's instructions (cat. no. C0016; Beyotime Institute of Biotechnology). The percentage of apoptotic cells was calculated as follows: $(OD_{sample\ well}-OD_{negative\ control\ well})/(OD_{positive\ control\ well}-OD_{negative\ control\ well})$ x100%.

Reverse transcription-quantitative PCR (RT-qPCR). Total RNA was extracted from cerebral tissues of MCAO mice samples or BV-2 cells using TRIzol (CWbiotech, Co., Ltd.). Reverse transcription was performed using the PrimeScript™ RT Master Mix (Takara Bio, Inc.). miRNA was extracted using the miRcute Isolation Kit (Tiangen Biotech Co., Ltd.) and reverse transcription was conducted using the miScript II RT Kit (Qiagen GmbH). qPCR was performed using the FastSYBR Mixture (cat. no. CW0955; CWbiotech, Co., Ltd.). The relative expression levels were analyzed using the $2^{-\Delta\Delta Cq}$ method (20). 18S RNA and U6 were used as the internal control. The amplification conditions for RT-PCR were as follows: 42˚C for 40 min, followed by 85˚C for 5 min. The amplification conditions for qPCR were as follows: 95˚C for 10 min, followed by 40 cycles each at 95˚C for 15 sec, 60˚C for 30 sec, and 72˚C for 30 sec. The primers used were as follows: XIST forward, 5'-TAAGGACTACTTAACGGGCT-3'and reverse, 5'-TACTCAGACATTCCCTGGCA-3'; miR-96-5p forward, 5'-TTTGGCACTAGCACATTTTTGCT-3' and reverse, 5'-GTGCAGGGTCCGAGGT-3'; IKKβ forward, 5'-GACATCGCATCGGCTCTTAGA-3' and reverse, 5'-AACGGTCACGGTGTACTTCTG-3'; U6 forward, 5'-CTCGCTTCGGCAGCACATATACT-3' and reverse, 5'-ACGCTTCACGAATTTGCGTGTC-3' and 18S forward, 5'-GTAACCCGTTGAACCCCATT-3' and reverse, 5'-CCATCCAATCGGTAGTAGCG-3'.

Western blotting. Total proteins were isolated from cell samples using RIPA lysis buffer (Beyotime Institute of Biotechnology). Protein concentration determination was performed using a BCA Protein Assay Kit (Takara Bio, Inc.). A total of 20 μg of protein was electrophoresed on 10% SDS-PAGE gels and then transferred onto PVDF membranes; PVDF membranes were then blocked with 5% BSA (Beijing Solarbio Science & Technology Co., Ltd.) at room temperature for 40 min. Thereafter, the membrane was then incubated overnight at 4˚C with anti-IKKβ (1:1,000; cat. no. ab109749; Abcam), anti-phosphorylated (p)-p65 (Ser536) (1:1,000; cat. no. 3033; Cell Signaling Technology, Inc.), and anti-p65 antibodies (1:1,000; cat. no. 8242; Cell Signaling Technology, Inc.), followed by incubation with horseradish peroxidase-conjugated anti-rabbit IgG antibody (1:1,000; cat. no. 7074; Cell Signaling Technology, Inc.). The protein expression levels were measured by an enhanced chemiluminescence detection kit (Thermo Fisher Scientific, Inc.). To quantify the protein expression, ImageJ 1.8.0 software (National Institutes of Health) was used to analyze the gray value of the protein bands.

Non-coding RNA target prediction and dual-luciferase reporter assay. The putative interaction between lncRNA XIST and miR-96-5p was searched by starBase v3.0 (http://starbase.sysu.edu.cn/) website and the target gene of miR-96-5p was predicted in TargetScan 7.2 (http://www.targetscan.org/). The p-NF-κB-Luc plasmid with the NF-κB response element cloned into Firefly pGL6 (Beyotime Institute of Biotechnology) and the *Renilla* pRL-TK plasmid (internal control; Promega Corporation) were used as luciferase reporter vectors. 293T cells were purchased from the The Cell Bank of Type Culture Collection of the Chinese Academy of Sciences and cultured in DMEM with 10% FBS, 100 μg/ml streptomycin and penicillin at 37˚C and 5% CO_2. The vectors (50 ng for each vector), combined with miRNA mimic/inhibitor or corresponding negative controls (20 nM for each miRNA mimic/inhibitor or controls), were co-transfected into 293T cells using Lipofectamine 2000 (Invitrogen; Thermo Fisher Scientific, Inc.). Then, 24 h later, the cells were collected and the luciferase activities were assessed using the Dual-luciferase Reporter Assay Kit (Promega Corporation).

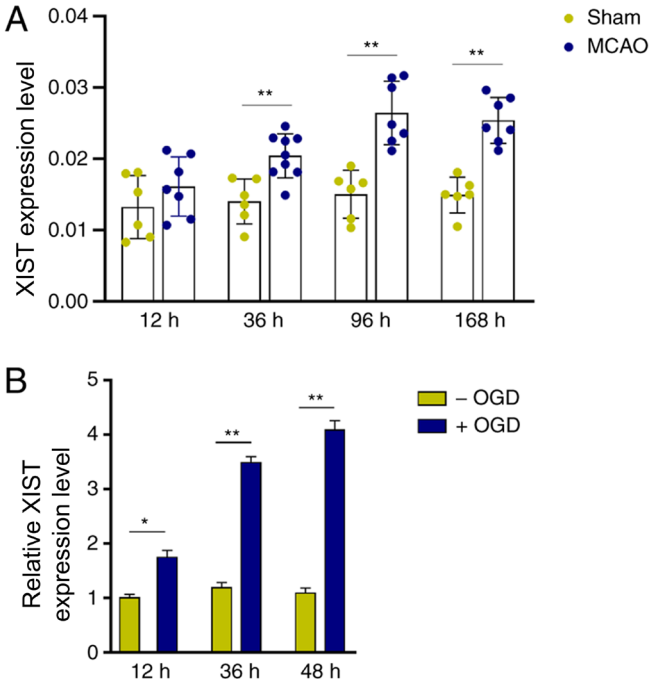

Figure 1. LncRNA XIST is upregulated in MCAO-treated mice and OGD-activated microglia. (A) XIST mRNA levels in mouse brain tissues were examined by qPCR 12, 36, 96 and 168 h after MCAO or sham treatment. (B) XIST mRNA levels in BV-2 microglial cells treated with OGD for 12, 36 and 48 h were examined by qPCR. *P<0.05 and **P<0.01. LncRNA long non-coding RNA; XIST, X-inactive specific transcript; MCAO, middle cerebral artery occlusion; OGD, oxygen/glucose deprivation; qPCR, quantitative PCR.

Statistical analysis. All quantitative data were expressed as the mean ± SD. GraphPad Prism 7 (GraphPad Software, Inc.) was used for statistical analysis in the present study. Unpaired Student's t-test was employed to compare two groups. Comparison among multiple groups was measured with one-way ANOVA followed by Tukey's post hoc test. P<0.05 was considered to indicate a statistically significant difference. Correlation analysis was conducted using Spearman's rank correlation coefficient.

Results

LncRNA XIST is upregulated in MCAO mice and OGD-activated microglia. To profile the expression of XIST in cerebral infarction, an *in vivo* mouse MCAO ischemic model

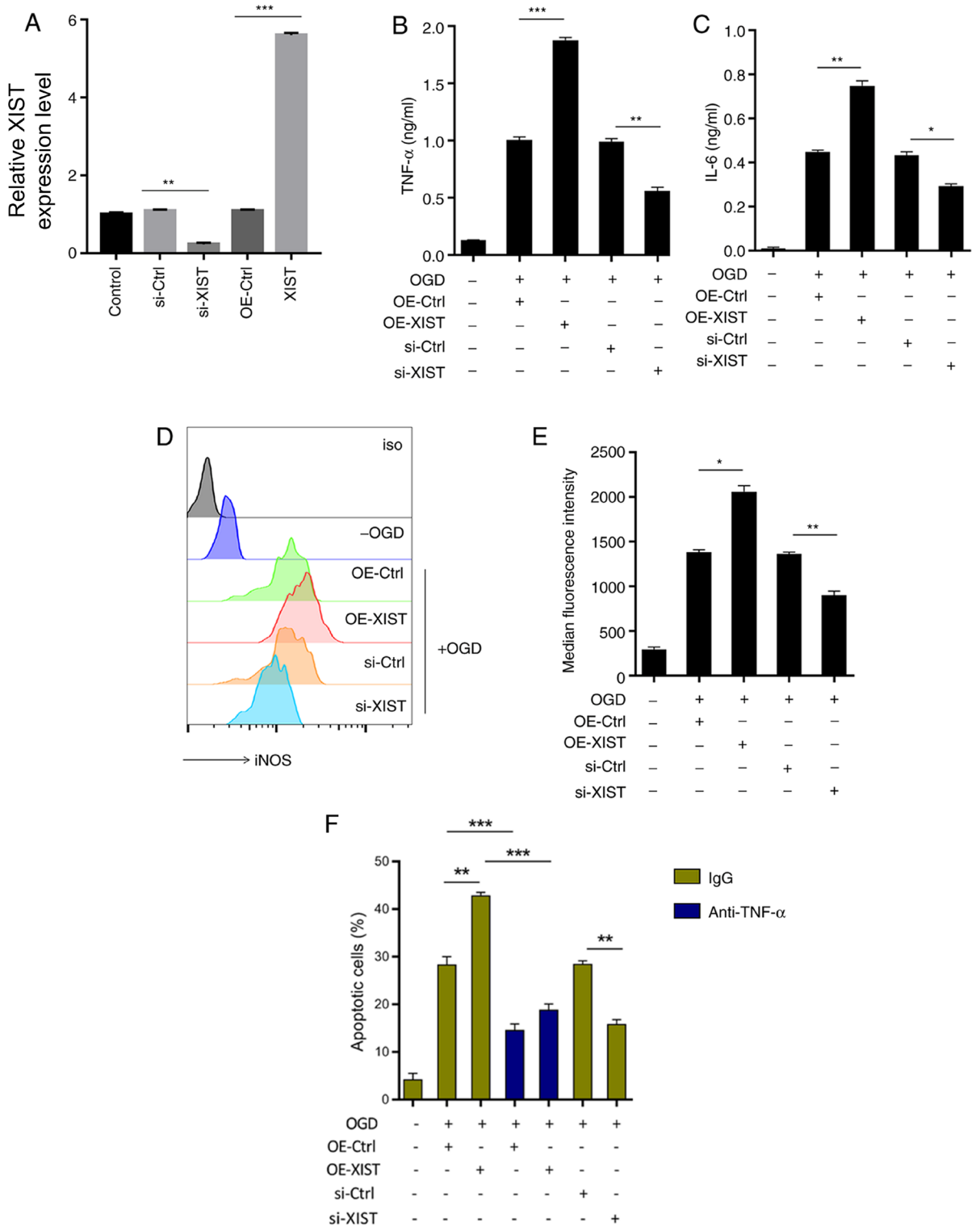

Figure 2. XIST promotes the release of proinflammatory cytokines and controls TNF-α-mediated neuronal apoptosis. After transfection with the XIST overexpression vector, siRNA or corresponding controls, BV-2 cells were exposed to OGD for 24 h. (A) Confirmation of knockdown and overexpression of XIST by reverse transcription-quantitative PCR. (B) TNF-α and (C) IL-6 expression levels in the culture supernatants were assayed by ELISA. iNOS expression in the BV-2 cells was assessed by (D) flow cytometry and expressed as (E) median fluorescence intensity. (F) Apoptosis of mouse primary cerebral neurons was examined using a lactate dehydrogenase assay after incubation with the culture supernatants containing TNF-α neutralization antibody or IgG control. *P<0.05, **P<0.01 and ***P<0.001. XIST, X-inactive specific transcript; TNF, transforming growth factor; IL, interleukin; iNOS, inducible nitric oxide synthase; si-, small interfering; Ctrl, control; OE, overexpression.

was established. Compared with the sham group, XIST expression was significantly increased in mouse cerebral tissues 36 h after MCAO treatment, and this upregulation could also be observed 168 h after MCAO treatment (Fig. 1A). Furthermore, it was observed that the *in vitro* OGD treatment significantly increased XIST expression in BV-2 cells in a time-dependent

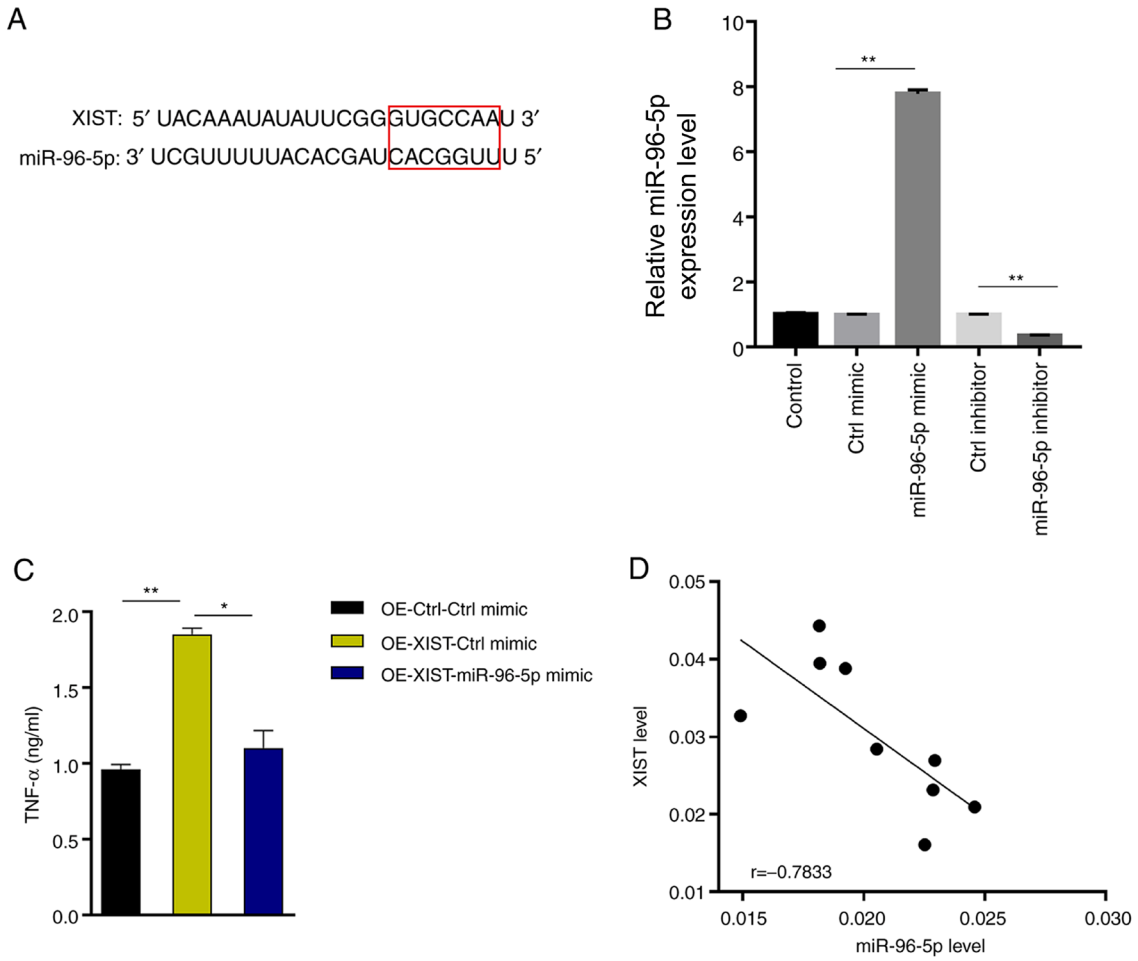

Figure 3. XIST enhances TNF-α production by directly suppressing miR-96-5p. (A) Direct interaction between XIST and miR-96-5p (shown in the red rectangle) predicted in the starBase database. (B) Confirmation of knockdown and overexpression of miR-96-5p by reverse transcription-quantitative PCR. (C) TNF-α release from OGD-induced BV-2 cells was assessed by ELISA after XIST overexpression and miR-96-5p mimic (or control) transfection. (D) The correlation between the mRNA levels of XIST and miR-95-5p was analyzed by the Spearman's rank correlation coefficient. *P<0.05 and **P<0.01. XIST, X-inactive specific transcript; TNF, transforming growth factor; miR-96-5p, microRNA-96-5p; OGD, oxygen/glucose deprivation; Ctrl, control; OE, overexpression.

manner (Fig. 1B). These results suggested that lncRNA XIST may be involved in the pathological process of cerebral infarction by modulating microglial function.

LncRNA XIST promotes pro-inflammatory mediator production and mediates TNF-α-mediated neuronal apoptosis. To investigate the role of lncRNA XIST in microglia-mediated neuroinflammation, TNF-α and IL-6 were examined after altering XIST expression (Fig. 2A-C). Fig. 2A demonstrated the transfection efficiency of si-XIST and XIST overexpression XIST in microglia. XIST overexpression enhanced the production of TNF-α (1.8-fold increase) and IL-6 (1.68-fold increase) in OGD-challenged microglia (Fig. 2B and C). However, XIST inhibition downregulated the levels of TNF-α (45% decrease) and IL-6 (14% decrease) (Fig. 2B and C). Similarly, OGD-induced iNOS expression was augmented (1.45-fold increase) by XIST overexpression, but was attenuated (34% decrease) after XIST inhibition (Fig. 2D and E).

Compared with neurons grown in the supernatants of OGD-BV-2 cells, culture supernatant from XIST-overexpressed OGD-BV-2 cells exacerbated neuronal apoptosis (1.5-fold increase), while TNF-α neutralization rescued this effect (50% decrease) (Fig. 2F). Compared with the OGD-BV-2 cell supernatant culture, the lncRNA XIST-silenced OGD-BV-2 cell supernatant significantly inhibited neuronal apoptosis (45% decrease; Fig. 2F). These results indicated that lncRNA XIST contributed to TNF-α-mediated neuronal apoptosis by promoting microglial proinflammatory activation.

LncRNA XIST enhances TNF-α production by directly suppressing miR-96-5p. To further elucidate the underlying molecular mechanism of lncRNA XIST function, the starBase website was searched and a putative interaction between lncRNA XIST and miR-96-5p (Fig. 3A) was found. miR-96-5p was successfully knocked down or overexpressed in BV-2 cells (Fig. 3B). miR-96-5p overexpression antagonized the ability of XIST to enhance TNF-α production (37% decrease, OE-XIST + miR-96-5p mimic vs. OE-XIST + Ctrl mimic; Fig. 3C). Further analysis of the expression profiles revealed a negative correlation between lncRNA XIST and miR-96-5p in MCAO-treated mouse brain tissues (Fig. 3D), indicating that XIST acts as a sponge for miR-96-5p to antagonize its function.

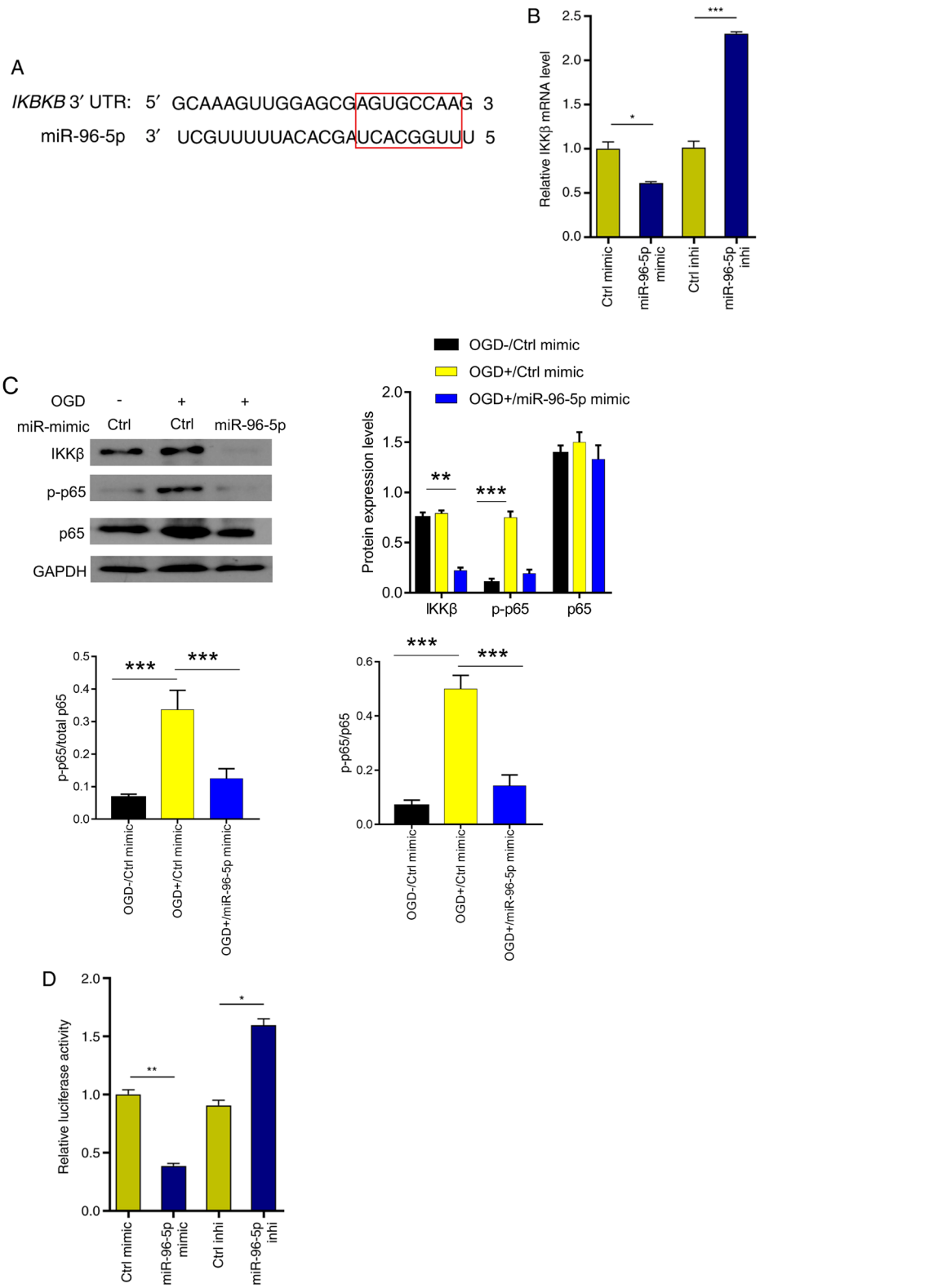

Figure 4. miR-96-5p inactivates NF-κB signaling by targeting and inhibiting IKKβ. (A) IKKβ was predicted to be a target of miR-96-5p in starBase (the red rectangle indicates the binding sequence). (B) IKKβ mRNA levels were examined after transfection with miR-96-5p mimic, inhibitor or control. (C) Immunoblots of IKKβ, p65, and p-p65 proteins in OGD-induced BV-2 cells after transfection with miR-96-5p mimic or control. (D) The luciferase activities were determined at 24 h after cotransfection of p-NF-κB-Luc plasmid, *Renilla* pRL-TK plasmid (internal control), and miR-96-5p mimic/inhibitor or corresponding negative controls into 293 cells. *P<0.05, **P<0.01 and ***P<0.001. miR-96-5p, microRNA-96-5p; IKKβ, inhibitor of nuclear factor κB kinase subunit β; p-, phosphorylated; Ctrl, control; OGD, oxygen/glucose deprivation.

MiR-96-5p downregulates NF-κB signaling and reduces TNF-α production by inhibiting IKKβ expression. Next, the target gene of miR-96-5p was predicted in TargetScan and it was revealed that miR-96-5p could directly bind to the IKKβ (Fig. 4A), whose activation is a vital event upstream of NF-κB signaling (21,22). To validate this, miR-96-5p mimic or

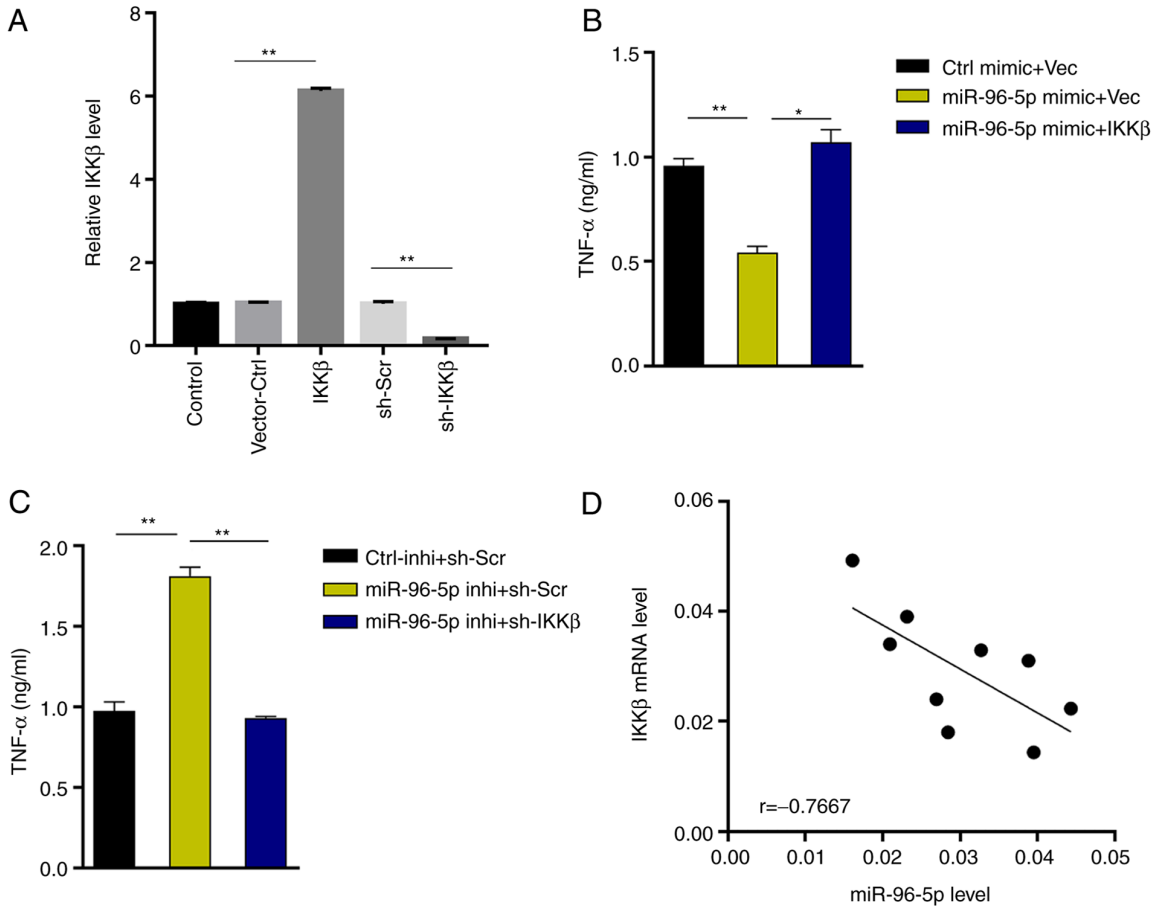

Figure 5. miR-96-5p reduces TNF-α production by inhibiting IKKβ expression. (A) Reverse transcription-quantitative PCR was used for confirmation of knockdown and overexpression of IKKβ. (B) miR-96-5p mimic reduced TNF-α release from OGD-treated BV-2 cells, while IKKβ overexpression rescued this effect. (C) miR-96-5p inhibitor enhanced TNF-α release from OGD-treated BV-2 cells while IKKβ inhibition counteracted this effect. (D) miR-96-5p was negatively correlated with IKKβ in middle cerebral artery occlusion-treated mouse cerebral tissues. Spearman's rank correlation coefficient was used. *P<0.05 and **P<0.01. miR-96-5p, microRNA-96-5p; TNF, tumor necrosis factor; IKKβ, inhibitor of nuclear factor κB kinase subunit β; OGD, oxygen/glucose deprivation; Ctrl, control; sh-, short hairpin.

inhibitor was transfected into microglia, and IKKβ expression was examined using RT-qPCR. The results revealed that IKKβ expression was significantly inhibited by miR-96-5p overexpression (41% decrease; Fig. 4B). In contrast, IKKβ expression was significantly enhanced upon miR-96-5p inhibition (2.3-fold increase) (Fig. 4B). At the protein level, miR-96-5p overexpression downregulated the expression of IKKβ (47% decrease), and thus decreased the level of p-p65 (the active subunit of NF-κB) (75% decrease), which was upregulated by OGD treatment (Fig. 4C). In addition, compared with the OGD+/Ctrl mimic group (p-p65/total p65=0.44), miR-96-5p overexpression significantly reduced the ratio of p-p65/total p65 (p-p65/total p65=0.16) (Fig. 4C). In order to further verify the miR-96-5p/IKKβ interaction, miR-96-5p mimic/inhibitor and NF-κB luciferase reporter were co-transfected into 293 cells. Luciferase activity was decreased upon miR-96-5p overexpression (63% decrease), but increased upon miR-96-5p inhibition (1.8-fold increase) (Fig. 4D). These results indicated that miR-96-5p downregulated NF-κB signaling by suppressing IKKβ expression.

To further substantiate the results, a rescue assay was performed. IKKβ was successfully knocked down or overexpressed in BV-2 cells (Fig. 5A). The results revealed that IKKβ overexpression reversed the decreased TNF-α production in miR-96-5p mimic-transfected microglia (2.1-fold increase, miR-96-5p mimic + IKKβ vs. miR-96-5p mimic + Vec), while IKKβ silencing inhibited the upregulation of TNF-α production in miR-96-5p inhibitor-transfected microglia (48% decrease, miR-96-5p inhibitor + sh-IKKβ vs. miR-96-5p inhibitor + sh-Scr) (Fig. 5B and C). Furthermore, IKKβ expression was inversely associated with miR-96-5p expression in MCAO-treated mouse brain tissues (Fig. 5D), supporting the IKKβ-targeting role of miR-96-5p.

TNF-α in turn positively regulates lncRNA XIST expression. Finally, the possible factors that contributed to the augmented XIST expression in microglia were investigated. Notably, it was determined that TNF-α stimulation significantly upregulated XIST expression in microglia in the absence of OGD treatment (4.2-fold increase) (Fig. 6). Concordant with this, the TNF-α neutralizing antibody counteracted OGD-induced enhancement of XIST expression (47% decrease) (Fig. 6). Collectively, these results indicated that lncRNA XIST supported the expression of TNF-α, which in turn positively regulated XIST expression in microglia and thus formed a feedback to promote the proinflammatory activation of microglia.

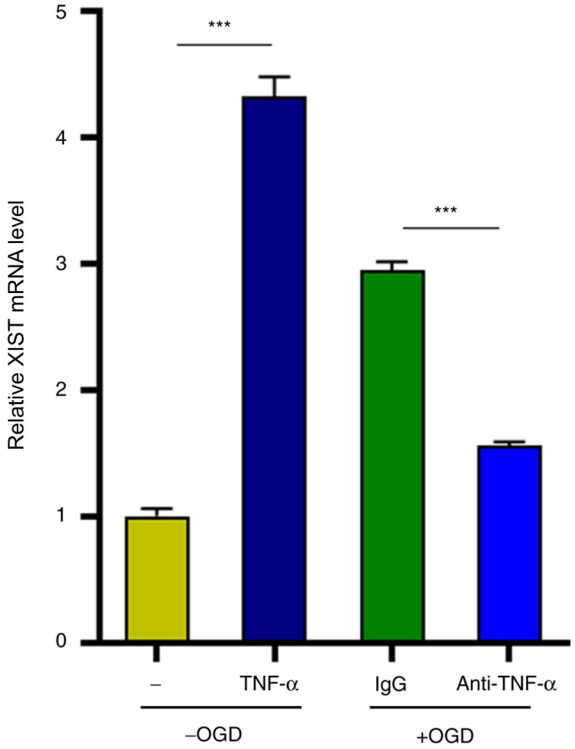

Figure 6. TNF-α positively regulates XIST expression. XIST mRNA levels in BV-2 cells were examined using reverse transcription-quantitative PCR after treatment with TNF-α (5 ng/ml), OGD and the TNF-α neutralization antibody, or with OGD and the IgG control. ***P<0.001. TNF, tumor necrosis factor; XIST, X-inactive specific transcript; OGD, oxygen/glucose deprivation.

Discussion

In the present study, it was revealed that lncRNA XIST was significantly upregulated in MCAO-treated mice and OGD-treated microglia. In addition, it was also demonstrated that XIST overexpression enhanced the expression and release of pro-inflammatory mediators in microglia. LncRNA XIST has been reported to participate in multiple diseases, including cancer and neurological diseases (16,23-26). In spinal cord injury, XIST promoted neuronal apoptosis by regulating AKT phosphorylation (16). In the cellular model of Alzheimer's disease, lncRNA XIST was involved in oxidative stress and apoptosis of hippocampal neurons by functioning as a sponge for miR-132 (27). In line with this, data from GEO database revealed that XIST expression in a patient was augmented within 6 months after ischemic stroke (28). However, the regulatory mechanism of XIST on the inflammatory polarization of microglia in cerebral infarction remains unclear.

Inflammation plays an important role in the pathophysiological process of cerebral infarction and has a dual role of protection and harm to the brain tissue. LncRNA XIST was confirmed to promote neuroinflammation by promoting the expression of TNF-α and IL-6 (28). Downregulation of XIST repressed inflammatory cytokine expression (approximately 60% decrease for COX-2, 50% decrease for TNF-α and IL-6) in microglias (26). XIST silencing was revealed to counteract LPS-induced TNF-α and IL-6 production (approximately 60% decrease for TNF-α and IL-6) in microglial cells (29). The present research revealed that XIST knockdown inhibited pro-inflammatory mediator production (45% decrease for TNF-α, 14% decrease for IL-6, and 34% decrease for iNOS) and TNF-α-mediated neuronal apoptosis (45% decrease). These results were consistent with previous research results (26,28,29). To investigate the regulatory mechanism of lncRNA XIST, the miRNAs that bind to it were explored and it was revealed that XIST could act as a sponge for miR-96-5p, counteracting its inhibitory effect on TNF-α production. The present research revealed that miR-96-5p overexpression repressed TNF-α production (37% decrease). A previous study revealed that downregulation of miR-96 markedly increased the level of TNF-α in BV2 cells (approximately 2.0-fold increase) (30). miR-96-5p has an inhibitory effect on autophagy and apoptosis of breast tumor cells (31). Kinoshita *et al* revealed that the diurnal rhythm of miR-96-5p played a protective role in dopaminergic neurons in Parkinson's disease (32). Collectively, these studies and our findings indicate the crucial role of miR-96-5p in neurological diseases and neuronal apoptosis.

IKKβ/IkB/NF-κB signaling plays a protective or toxic role in neuroinflammation depending on the differential external stimuli, cell types, and activation of NF-κB dimers (33,34). Microglial activation of the NF-κB p50/p65 subunit downstream of IKKβ was correlated with the production of pro-inflammatory mediators, including IFN-γ, TNF-α, and IL-6, resulting in secondary injury after the initial onset of cerebral infarction (21,33). A previous study showed that targeting XIST induced apoptosis of human osteosarcoma cells by activating NF-κB (35). Another previous study revealed that miR-96 overexpression directly inhibits IKKβ expression, but the upstream regulation of miR-96 has not been explored (30). The present results revealed that IKKβ was directly targeted and silenced by miR-96-5p. It was also revealed that p-p65 (the active subunit of NF-κB) accompanied by pro-inflammatory cytokines was downregulated (75% decrease) accordingly when miR-96-5p was overexpressed, demonstrating the modulation of lncRNA XIST/miR-96-5p on IKKβ/IkB/NF-κB signaling in microglia. IKKβ silencing inhibited TNF-α production (48% decrease), which was consistent with a previous study (IKKβ silencing resulted in a decrease in the TNF-α level of approximately 35%) (30). Notably, it was revealed that TNF-α, whose production could be induced by the upstream lncRNA XIST/miR-96-5p/IKKβ/NF-κB axis, which in turn augmented XIST expression (4.2-fold increase), indicating that there could be a positive feedback loop between XIST and TNF-α production through miR-96-5p/IKKβ/NF-κB signaling. In the future, the detailed modulation mechanism of the positive feedback loop between XIST and TNF-α in cerebral infarction remains to be elucidated.

In conclusion, it was revealed that the lncRNA XIST promoted inflammatory polarization of microglia in cerebral ischemia by regulating the miR-96-5p/IKKβ/NF-κB axis, leading to enhanced production of proinflammatory mediators and aggravated neuronal apoptosis. The lncRNA XIST may be a potential target in lncRNA-based ischemia therapy. The present findings provide novel insights into the functional involvement of microglia in cerebral infarction and its modulation mechanism.

Acknowledgements

Not applicable.

Funding

This study was supported by the Youth Grant from the Science Foundation of Hebei Province (grant no. H2018206232).

Availability of data and materials

The datasets used and/or analyzed during the present study are available from the corresponding author on reasonable request.

Authors' contributions

MZ and JKY designed the original research. MZ conducted the statistical analysis and drafted the manuscript. MZ, JKY and JM participated in the data collection and interpretation. All authors read and approved the final manuscript. MZ and JKY can authenticate the raw data in this study.

Ethics approval and consent to participate

The experiments were carried out in accordance with the National Institutes of Health (NIH) guidelines for the care and use of laboratory animals approved by the Animal Ethics Committee of Xingtai Medical College Second Affiliated Hospital (Xingtai China).

Patient consent for publication

Not applicable.

Competing interests

The authors declare that they have no competing interests.

References

1. Lozano R, Naghavi M, Foreman K, Lim S, Shibuya K, Aboyans V, Abraham J, Adair T, Aggarwal R, Ahn SY, *et al*: Global and regional mortality from 235 causes of death for 20 age groups in 1990 and 2010: A systematic analysis for the global burden of disease study 2010. Lancet 380: 2095-2128, 2012.
2. Wang C, Li N, Wang H, Yin H, Zhao Y: Study on essential drug use status and its influencing factors among cerebral infarction inpatients in county level hospitals of Anhui Province, China. PLoS One 13: e0193513, 2018.
3. Holliday EG, Traylor M, Malik R, Bevan S, Falcone G, Hopewell JC, Cheng YC, Cotlarciuc I, Bis JC, Boerwinkle E, *et al*: Genetic overlap between diagnostic subtypes of ischemic stroke. Stroke 46: 615-619, 2015.
4. Puthanveetil P, Chen S, Feng B, Gautam A and Chakrabarti S: Long non-coding RNA MALAT1 regulates hyperglycaemia induced inflammatory process in the endothelial cells. J Cell Mol Med 19: 1418-1425, 2015.
5. Benakis C, Garcia-Bonilla L, Iadecola C and Anrather J: The role of microglia and myeloid immune cells in acute cerebral ischemia. Front Cell Neurosci 8: 461, 2015.
6. Seifert HA and Pennypacker KR: Molecular and cellular immune responses to ischemic brain injury. Transl Stroke Res 5: 543-553, 2014.
7. Faustino JV, Wang X, Johnson CE, Klibanov A, Derugin N, Wendland MF and Vexler ZS: Microglial cells contribute to endogenous brain defenses after acute neonatal focal stroke. J Neurosci 31: 12992-13001, 2011.
8. Hu X, Li P, Guo Y, Wang H, Leak RK, Chen S, Gao Y and Chen J: Microglia/macrophage polarization dynamics reveal novel mechanism of injury expansion after focal cerebral ischemia. Stroke 43: 3063-3070, 2012.
9. Orihuela R, McPherson CA and Harry GJ: Microglial M1/M2 polarization and metabolic states. Br J Pharmacol 173: 649-665, 2016.
10. Tang Y and Le W: Differential roles of M1 and M2 microglia in neurodegenerative diseases. Mol Neurobiol 53: 1181-1194, 2016.
11. Bao MH, Szeto V, Yang BB, Zhu SZ, Sun HS and Feng ZP: Long non-coding RNAs in ischemic stroke. Cell Death Dis 9: 281, 2018.
12. Ren W and Yang X: Pathophysiology of long non-coding RNAs in ischemic stroke. Front Mol Neurosci 11: 96, 2018.
13. Dykstra-Aiello C, Jickling GC, Ander BP, Shroff N, Zhan X, Liu D, Hull H, Orantia M, Stamova BS and Sharp FR: Altered expression of long noncoding RNAs in blood after ischemic stroke and proximity to putative stroke risk loci. Stroke 47: 2896-2903, 2016.
14. Yan H, Rao J, Yuan J, Gao L, Huang W, Zhao L and Ren J: Long non-coding RNA MEG3 functions as a competing endogenous RNA to regulate ischemic neuronal death by targeting miR-21/PDCD4 signaling pathway. Cell Death Dis 8: 3211, 2017.
15. Wang J, Zhao H, Fan Z, Li G, Ma Q, Tao Z, Wang R, Feng J and Luo Y: Long noncoding RNA H19 promotes neuroinflammation in ischemic stroke by driving histone deacetylase 1-dependent M1 microglial polarization. Stroke 48: 2211-2221, 2017.
16. Gu S, Xie R, Liu X, Shou J, Gu W and Che X: Long coding RNA XIST contributes to neuronal apoptosis through the downregulation of AKT phosphorylation and is negatively regulated by miR-494 in rat spinal cord injury. Int J Mol Sci 18: 732, 2017.
17. Xu LX, Lv Y, Li YH, Ding X, Wang Y, Han X, Liu MH, Sun B and Feng X: Melatonin alleviates brain and peripheral tissue edema in a neonatal rat model of hypoxic-ischemic brain damage: The involvement of edema related proteins. BMC Pediatr 17: 90, 2017.
18. Blanco S, Hernández R, Franchelli G, Ramos-Álvarez MM and Peinado MÁ: Melatonin influences NO/NOS pathway and reduces oxidative and nitrosative stress in a model of hypoxic-ischemic brain damage. Nitric Oxide 62: 32-43, 2017.
19. Ni J, Wang X, Chen S, Liu H, Wang Y, Xu X, Cheng J, Jia J and Zhen X: MicroRNA let-7c-5p protects against cerebral ischemia injury via mechanisms involving the inhibition of microglia activation. Brain Behav Immun 49: 75-85, 2015.
20. Livak KJ and Schmittgen TD: Analysis of relative gene expression data using real-time quantitative PCR and the 2(-Delta Delta C(T)) method. Methods 25: 402-408, 2001.
21. Ridder DA and Schwaninger M: NF-kappaB signaling in cerebral ischemia. Neuroscience 158: 995-1006, 2009.
22. Herrmann O, Baumann B, de Lorenzi R, Muhammad S, Zhang W, Kleesiek J, Malfertheiner M, Köhrmann M, Potrovita I, Maegele I, *et al*: IKK mediates ischemia-induced neuronal death. Nat Med 11: 1322-1319, 2005.
23. Zhang YL, Li XB, Hou YX, Fang NZ, You JC and Zhou QH: The lncRNA XIST exhibits oncogenic properties via regulation of miR-449a and Bcl-2 in human non-small cell lung cancer. Acta Pharmacol Sin 38: 371-381, 2017.
24. Yao Y, Ma J, Xue Y, Wang P, Li Z, Liu J, Chen L, Xi Z, Teng H, Wang Z, *et al*: Knockdown of long non-coding RNA XIST exerts tumor-suppressive functions in human glioblastoma stem cells by up-regulating miR-152. Cancer Lett 359: 75-86, 2015.
25. Jin H, Du XJ, Zhao Y and Xia DL: XIST/miR-544 axis induces neuropathic pain by activating STAT3 in a rat model. J Cell Physiol 233: 5847-5855, 2018.
26. Yan XT, Lu JM, Wang Y, Cheng XL, He XH, Zheng WZ, Chen H and Wang YL: XIST accelerates neuropathic pain progression through regulation of miR-150 and ZEB1 in CCI rat models. J Cell Physiol 233: 6098-6106, 2018.
27. Wang X, Wang C, Geng C and Zhao K: LncRNA XIST knockdown attenuates $A\beta_{25-35}$-induced toxicity, oxidative stress, and apoptosis in primary cultured rat hippocampal neurons by targeting miR-132. Int J Clin Exp Pathol 11: 3915-3924, 2018.
28. Li WX, Qi F, Liu JQ, Li GH, Dai SX, Zhang T, Cheng F, Liu D and Zheng SG: Different impairment of immune and inflammation functions in short and long-term after ischemic stroke. Am J Transl Res 9: 736-745, 2017.

29. Zhao Q, Lu F, Su Q, Liu Z, Xia X, Yan Z, Zhou F and Qin R: Knockdown of long noncoding RNA XIST mitigates the apoptosis and inflammatory injury of microglia cells after spinal cord injury through miR-27a/Smurf1 axis. Neurosci Lett 715: 134649, 2020.
30. Huang Y, Zhu N, Chen T, Chen W, Kong J, Zheng W and Ruan J: Triptolide suppressed the microglia activation to improve spinal cord injury through miR-96/IKKβ/NF-κB pathway. Spine (Phila Pa 1976) 44: E707-E714, 2019.
31. Shi Y, Zhao Y, Shao N, Ye R, Lin Y, Zhang N, Li W, Zhang Y and Wang S: Overexpression of microRNA-96-5p inhibits autophagy and apoptosis and enhances the proliferation, migration and invasiveness of human breast cancer cells. Oncol Lett 13: 4402-4412, 2017.
32. Kinoshita C, Aoyama K, Matsumura N, Kikuchi-Utsumi K, Watabe M and Nakaki T: Rhythmic oscillations of the microRNA miR-96-5p play a neuroprotective role by indirectly regulating glutathione levels. Nat Commun 5: 3823, 2014.
33. Schneider A, Martin-Villalba A, Weih F, Vogel J, Wirth T and Schwaninger M: NF-kappaB is activated and promotes cell death in focal cerebral ischemia. Nat Med 5: 554-559, 1999.
34. Shih RH, Wang CY and Yang CM: NF-kappaB signaling pathways in neurological inflammation: A mini review. Front Mol Neurosci 8: 77, 2015.
35. Gao W, Gao J, Chen L, Ren Y and Ma J: Targeting XIST induced apoptosis of human osteosarcoma cells by activation of NF-kB/PUMA signal. Bioengineered 10: 261-270, 2019.